INTERNATIONAL JOURNAL OF OPTIMIZATION IN CIVIL ENGINEERING
Int. J. Optim. Civil Eng., 2015; 5(4):493-509

OPTIMAL HYBRID BASE ISOLATION AND MR DAMPER

M. Mohebbi[*, †], H. Dadkhah, K. Shakeri
Faculty of Engineering, University of Mohaghegh Ardabili, 56199-11367, Ardabil, Iran

ABSTRACT

In this paper, optimal design of hybrid low damping base isolation and magnetorheological (MR) damper has been studied. Optimal hybrid base isolation system has been designed to minimize the maximum base drift of low damping base isolation system where for solving the optimization problem, genetic algorithm (GA) has been used. In design procedure the maximum acceleration of the structure has been limited, too. To determine the volatge of semi-active MR damper the H_2/LQG and clipped-optimal control algorithm has been applied. For numerical simulations, a three-story frame equipped with the hybrid base isolation and MR damper subjected to the scaled El Centro excitation and optimal hybrid system has been designed. Results of numerical simulations have proven the effectiveness of the optimal hybrid control system in controlling the maximum base drift of isolated structure. Also comparing the performance of hybrid, low and high damping base isolation systems has shown that adding MR damper to low damping base isolation system has improved its performance so that the hybrid system has worked better than high damping base isolation in reducing the maximum base drift. Testing optimal hybrid control system under different excitations has shown its efficiency.

Keywords: base isolation; hybrid base isolation; MR damper; base drift; clipped-optimal control.

Received: 10 March 2015; Accepted: 29 July 2015

1. INTRODUCTION

Base isolation systems are passive control systems that mitigate structural vibration and damage during seismic events. This kind of control system reduces structural acceleration and drift with shifting the period of structure. The shifted period increases the base drift of structure. Several alternatives could be used for adding the damping and decreasing the base

[*]Corresponding author: Faculty of Engineering, University of Mohaghegh Ardabili, 56199-11367. Ardabil, Iran
[†]E-mail address: mohebbi@uma.ac.ir (M. Mohebbi)

drift. Damping of the natural base isolation is about 2-3% of critical damping. One method for increasing the damping of base isolation is using the high damping natural rubber, natural rubber containing carbon black and other proprietary fillers that can increase the damping of base isolation up to 15-20% of critical damping [1]. Also leaden core in base isolation and supplemental dampers such as viscous dampers may be used to augment the damping [2]. Though these methods of increasing damping can reduce the base drift, these base isolation systems do not have the capability of adapting to different loading conditions. To solve this problem, blend of base isolation systems and active control system may be proposed that called hybrid control systems. Hybrid control systems can be effective for wide range of different loading conditions. Hybrid control systems have been investigated by a number of researchers [3-4] which the results indicate the advantages of hybrid base isolation systems such as high performance in mitigating structural vibration and the ability to adapt to wide range of ground excitation. Inaudi and Kelly investigated using active base isolation in a four-story building model employing an electro hydraulic actuator [3]. Also using sliding mode controller for buildings and bridge has been studied in previous researches [4-5]. Active base isolation systems need high external power supply during seismic events. To solve this problem, semi-active systems can be proposed instead the active systems to be used with the base isolation systems. Semi-active systems can adapt to different loading conditions and require low external power supply during the seismic events. Magneto-rheological damper (MR) damper is one of the semi-active control systems that has been investigated separately or in combination with the base isolation systems [6-10]. Ramallo et al. [11] experimentally demonstrated the effectiveness of semi-active base isolation in a two-story building and compared its performance with passive damper under far-field and near-field earthquake excitations, also Sanjay and Nagarajaiah [12] experimentally showed the effectiveness of MR damper and base isolation under near-field earthquake excitation.

In previous researches, the performance of hybrid system of base isolation and MR damper, especially comparing its efficiency with the high damping base isolation, has not been studied completely. Also optimization the performance of hybrid system in minimizing the response of structure, especially maximum base drift, and a detailed optimal design procedure has not been reported. Hence, in this paper, optimal design of base isolation and MR damper hybrid system is investigated to protect the building structures subjected to earthquake excitations where genetic algorithm (GA) is applied to solve the optimization problem. The main focus of this research is to demonstrate the potential of optimal low damping base isolation and MR damper in comparison with the high damping base isolation in mitigating the response of structure.

2. SYSTEM MODEL

Assuming the force provided by the MR damper and the period shifted by base isolation are adequate to keep the structure in the linear region. So the equation of motion of semi-active base isolation can be written

$$M_S\ddot{x} + C_S\dot{x} + K_S x = \Gamma f - M_s \Lambda \ddot{x}_g \tag{1}$$

where Γ=[-1 0 0 0]^T indicates the position of MR damper, f=the force of MR damper,Λ= a vector that all components are unity, x is the vector of the displacements of the structure relative to the ground and M_s, K_s and C_s are mass, stiffness and damping matrices of fixed-base and base isolation systems and $\ddot{x_g}$ is the ground acceleration.

The state-space form of the equation of motion is given by

$$\dot{Z} = AZ + Bf + E\ddot{x_g} \quad (2)$$

$$y = CZ + Df + v \quad (3)$$

where Z is the state vector (Z=[x $\dot{x}$]^T), y is the vector of measured outputs, v is the measurement noise vector and A, B, C and D are system matrices.

3. MR DAMPER MODEL

MR dampers are semi-active control devices that use magneto-rheological fluids to construct a versatile damping device. Base isolation systems can be adapted to wide range of ground excitation by adding MR damper even under near-field earthquake excitation that base isolation system is susceptible [13]. Dynamic behavior of MR damper depends to the voltage which currents in magneto-rheological fluid. The simple mechanical idealization of the MR damper is depicted in Fig. 1 [14].

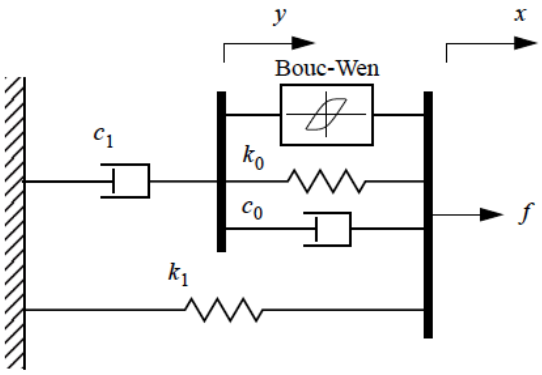

Figure 1. Simple mechanical model of the MR damper

The applied force predicted by this model is given as [14]:

$$f = az + c_0(\dot{x} - \dot{y}) + k_0(x - y) + k_1(x - x_0) \quad (4)$$

or equivalently

$$f = c_1\dot{y} + k_1(x - x_0) \quad (5)$$

$$\dot{z} = -\gamma|\dot{x} - \dot{y}|z|z|^{n-1} - \beta(\dot{x} - \dot{y})|z|^n + A(\dot{x} - \dot{y}) \quad (6)$$

$$\dot{y} = \frac{1}{c_1 + c_0}\{az + c_0\dot{x} + k_0(x - y)\} \tag{6}$$

where k_1, c_0 and c_1 represent the accumulator stiffness, the viscous damping and dashpot, respectively. Also $k_0$is present to control the stiffness at the large velocities,x_0 is the initial displacement of spring k_1 and the parameters γ, β and $A$are the parameters which used to define the shape of hysteresis loops.

The force of MR damper depends on the voltage that current in MR damper. Dyke et al. [15] have suggested the following equations to obtain the parameters of MR damper dynamic model:

$$a = a(u) = a_a + a_b u \tag{8a}$$
$$c_1 = c_1(u) = c_{1a} + c_{1b} u \tag{8b}$$
$$c_0 = c_0(u) = c_{0a} + c_{0b} u \tag{8c}$$

where u is given as the output of a first-order filter given by:

$$\dot{u} = -\eta(u - V) \tag{9}$$

V is the voltage that currents in MR damper and η is constant modulus with dimension Sec^{-1}.

4. CONTROL ALGORITHM

Two controllers are needed for controlling MR damper. The first controller calculates the optimum force and the second controller applies voltage of MR damper [16]. In this paper H_2/LQG (Linear Quadratic Gaussian) control is used to calculate the optimum force. This control can be used to mitigate the responses of hybrid system [17]. For designing of controller, $\ddot{x_g}$ is taken to be a stationary white noise. The regulated outputs are minimized using the following cost function:

$$J = \lim_{\tau\to\infty} \frac{1}{\tau} E\left[\int_0^{\tau} \left(\boldsymbol{z}^T(t)\boldsymbol{Q}\boldsymbol{z}(t) + r{f_c}^2\right)dt\right] \tag{10}$$

where Q and r are the weighting matrix and parameter. The elements of Q are determined according to the main purpose of designing of control system which in this research has been the minimization of the base drift.

The optimal control force is given as follows:

$$f_c = -k_c\bar{z} \tag{11}$$
$$\dot{\bar{z}} = A\bar{z} + Bf + L(y - C\bar{z} - Df) \tag{12}$$

Here k_c is the gain matrix for Linear Quadratic Regulator (LQR) and L is the gain matrix for

state estimator which is determined as:

$$k_c = \frac{\acute{B}P}{r} \tag{13}$$

$$L = (CS)^{\acute{}} \tag{14}$$

where P and S are the solution of the algebraic Ricatti equation given by:

$$PA + \acute{A}P - P\acute{B}BP/r + Q = 0 \tag{15}$$

$$S\acute{A} + AS - S\acute{C}CS + \gamma E\acute{E} = 0 \tag{16}$$

The force generated by MR damper depends on the response of structure. It is not always possible to generate the desired optimal force and in MR damper control system only the voltage can be directly changed. In this study the clipped-optimal control is used to apply the voltage of MR damper where the voltage is determined as [14]:

$$V = V_{max} H\{(f_c - f)f\} \tag{17}$$

Where V_{max} is the maximum voltage that can be applied to MR damper, and H{.} is the Heaviside step function. In the clipped-optimal control when the force produced by MR damper is smaller than the desired optimal force and two forces are the same sign, the voltage applied to MR damper is increased to the maximum level. Otherwise, the voltage applied is set to zero.

A block diagram of the clipped-optimal control is shown in Fig. 2.

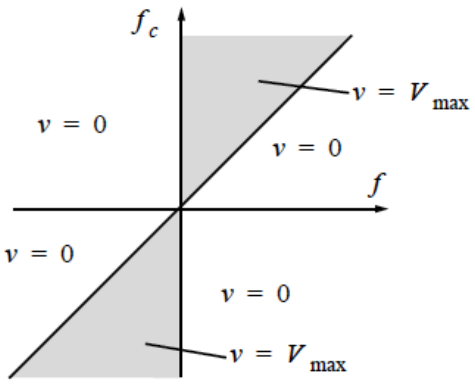

Figure 2. Diagram of clipped-optimal control system

A block diagram of the semi-active control system is shown in Fig. 3, where two different cases of fixed-base and base isolated structures have been considered.

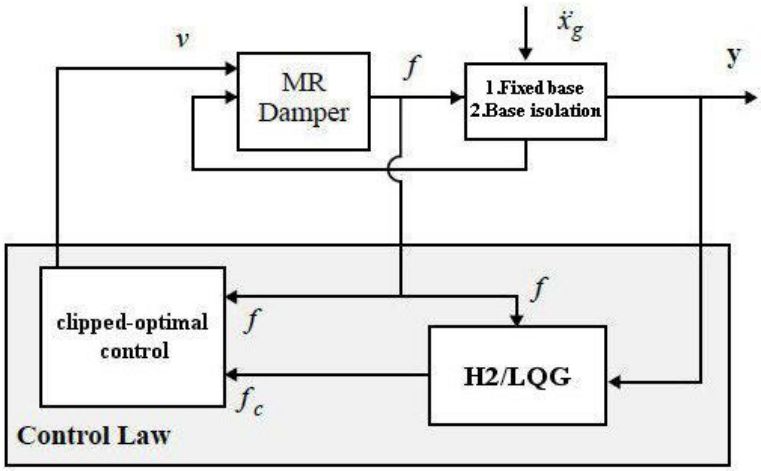

Figure 3. Diagram of semi-active control system

5. GENETIC ALGORITHM (GA)

Genetic algorithm is a method for optimization of problems based on natural selection. In GA individuals are selected randomly from the current population to produce the children for next generation.

Selection, crossover and mutation are three main operators of GA. In every generation, a set of chromosomes is selected for mating based on their relative fitness. This process of natural selection is operated by the selection operator. In this paper the stochastic universal sampling method [18] has been used for selecting a number of chromosomes for mating, based on their fitness values in the current population as:

$$P(\mathbf{x}_i)=\frac{F(\mathbf{x}_i)}{\sum_{i=1}^{N_{ind}} F(\mathbf{x}_i)},\ i=1,2,\ldots,N_{ind} \tag{18}$$

where $F(\mathbf{x}_i)$=fitness of chromosome $\mathbf{x}_i$ and $P(\mathbf{x}_i)$=probability of selection of x_i also N_{ind} = number of individuals.

Crossover produces new individuals that have some parts of both parents genetic material. In this paper the method proposed by Mühlenbein and Schlierkamp-Voosen [19] for crossover has been used, where each pair of parents can produce two newborns and each newborn can get its genes from either parent with equal probability as follows:

$$O=P_1+\alpha(P_2-P_1) \tag{19}$$

whereP_1 and P_2 are the parent chromosomes genes, O is the newborn gene, and α is a scaling factor chosen randomly over [-0.25, 1.25] interval typically. This method uses a new α for each pair of parents genes.

Mutation operator provides a guarantee that the probability of searching any given string

will never be zero.

In this paper the elitist strategy has been used where N_{elites} of the best chromosomes are selected as elites of the current generation to go to the next generation without modification. The rest of the chromosomes in the population are replaced by inserted newborns (N_{ins}). Hence:

$$N_{elites} = N_{ind} - N_{ins} \tag{20}$$

GA has been used successfully for solving optimization problems in different fields of civil engineering such as determination of optimal sensor locations for structural modal identification [20], optimization of the modal weights for nonlinear static analysis of structures [21] as well as optimal design of single and multiple tuned mass dampers as structural control systems [22-24].

6. NUMERICAL EXAMPLE

For numerical analysis, a three-story building model has been used which the structural models in both fixed-base and base isolation with MR damper configurations have been shown in Fig. 4.

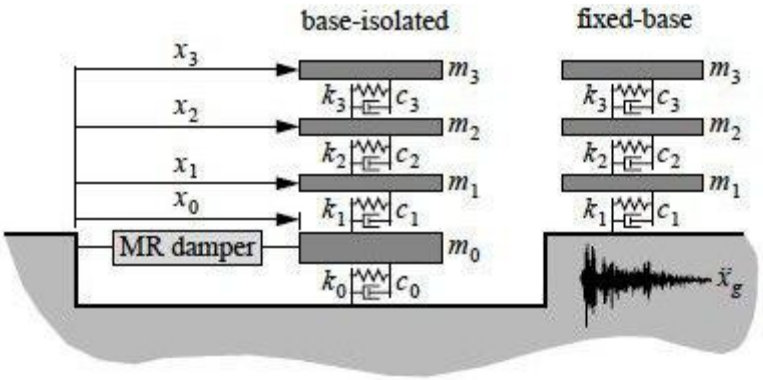

Figure 4. Model of the structure

The mass, stiffness and damping of the structure have been reported in Table 1[14]. In semi-active base isolation model, the structure on base isolation and fixed-base structure has the same properties.

Table 1: Parameters of fixed-base structure

Story	Floor masses (kg)	Stiffness coefficients $*10^5$ (N/m)	Damping coefficients (N.s/m)
1	98.3	5.16	125
2	98.3	6.84	50
3	98.3	6.84	50

In base isolated structure, one degree of freedom is added to dynamic model of the structure. The base massm_0 is chosen equal to the floor mass also the base stiffness k_0 is chosen such that the fundamental period of the base isolation structure is almost triple the fundamental period of the fixed-base structure [25]. The damping ratio of the base isolation is chosen as 15% of critical damping for the high damping base isolation and 2% for hybrid low damping base isolation and MR damper.

For numerical simulations a program has been developed using the MATLAB software. To verify the result of the numerical analysis, the output of the current research has been compared with the results of the experimental study conducted by Dyke et al. [14] and reported in Table 2. It is clear that an acceptable adaption has been achieved between the results.

Table 2. Verifying the written code in Matlab program

Control Strategy	Uncontrolled Structure		Clipped-Optimal Control	
	Dyke et al. [12]	Present Research	Dyke et al. [12]	Present Research
x_1	0.538	0.542	0.114	0.113
x_2	0.820	0.836	0.185	0.190
x_3	0.962	0.973	0.212	0.215
(cm)				
$\ddot{x}_1$	856	848	696	688
$\ddot{x}_2$	1030	1032	739	698
$\ddot{x}_3$	1400	1413	703	682
(cm/s^2)				
f(N)	-		941	923

The equation of motion of semi-active base isolation systems can be written in state space as follows:

$$\dot{Z} = AZ + Bf + E\ddot{x}_g \tag{21}$$

$$y = CZ + Df + v \tag{22}$$

when y is defined as the absolute acceleration of the base isolation and the structure floors and the displacement of base isolation (i.e. y=$[\ddot{x}_b \ddot{x}_1 \ddot{x}_2 \ddot{x}_3 x_b]^T$), the system matrices of Eq. (21) and (22) can be written as:

$$A=\begin{bmatrix} \mathbf{0}_{4\times4} & \mathbf{I}_{4\times4} \\ -\mathbf{M_S}^{-1}\mathbf{K_S} & -\mathbf{M_S}^{-1}\mathbf{K_S} \end{bmatrix},\quad B=\begin{bmatrix} \mathbf{0}_{4\times1} \\ \mathbf{M_S}^{-1}\boldsymbol{\Gamma} \end{bmatrix},\quad E=\begin{bmatrix} \mathbf{0}_{4\times1} \\ \boldsymbol{\Lambda}_{4\times1} \end{bmatrix},$$

$$C=\begin{bmatrix} -\mathbf{M_S}^{-1}\mathbf{K_S} & -\mathbf{M_S}^{-1}\mathbf{K_S} \\ 1\,0\,0\,0 & 0\,0\,0\,0 \end{bmatrix},\quad D=\begin{bmatrix} \mathbf{M_S}^{-1}\boldsymbol{\Gamma} \\ 0 \end{bmatrix},$$

The optimal parameters of MR damper used in this paper are given in Table 3 [14], also the capacity of MR damper and the maximum voltage has been 3000 (N) and 2.25 (v), respectively.

Table 3: Parameters of MR damper

Parameter	Value	Parameter	Value
c_{0a}	21 N.sec/cm	a_a	140 N/cm
c_{0b}	3.5 N.sec/cm.V	a_b	695 N/cm.V
k_0	46.9 N/cm	γ	363 cm^{-2}
c_{1a}	283 N.sec/cm	β	363 cm^{-2}
c_{1b}	2.95 N.sec/cm.V	A	301
k_1	5 N/cm	n	2
x_0	14.3 cm	η	190 sec^{-1}

The structure is subjected to the NS component of the 1940 El Centro earthquake shown in Fig. 5 where the earthquake is reproduced at five times the recorded rate.

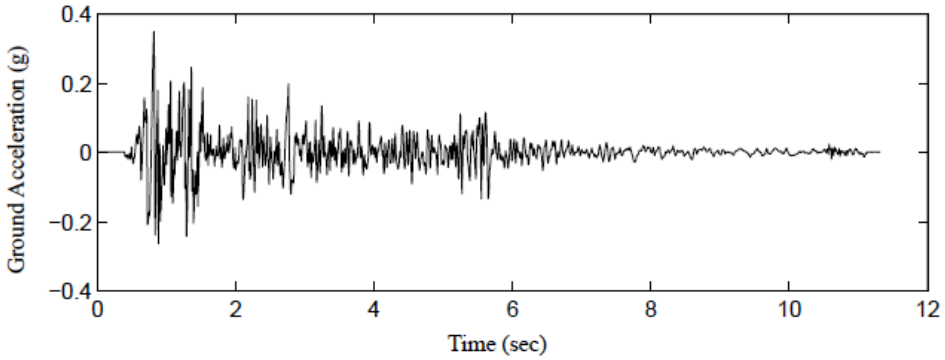

Figure 5. Time scaled NS component of the 1940 El Centro earthquake

In this paper, three cases have been investigated for MR damper and low damping base isolation system as follows:

Case (a): In this case the voltage of the MR damper has been constant (passive form) and the response of structure has been obtained for voltages 0.5, 1.5 and 2.25 (v).

Case (b): The voltage of the MR damper has been determined using theH_2/LQG and clipped-optimal control algorithm and the parameter *r* in Eq. (10) has been optimized using genetic algorithm without any constraints on structure or control system parameters.

Case (c): In this case, the voltage of the MR damper is determined similar to *Case (b)*while the maximum acceleration of the controlled structure is limited in solving the optimization problem. Finally, the performance of different control systems under the Northridge (PGA=0.58g, 1994) and the Tabas (PGA=0.85g, 1978) earthquakes has been tested.

6.1 Case (a): Base isolation and passive MR damper with constant voltage

In this case, the voltage of the MR damper has been constant; hence MR damper acts similar

to a passive control system. The maximum response of uncontrolled and controlled structures has been reported in Table 4 for different voltages of 0.5, 1.5 and 2.25 (v)when the structure subjected to the scaled El Centro excitation where $x_b, d_b \; and \; \ddot{x}_b$ are displacement, drift and absolute acceleration of the base isolation. $x_i, d_i \; and \; \ddot{x}_i$are displacement, drift and absolute acceleration of the i^{th} floor and f is MR damper force.

Table 4: Peak response of uncontrolled and controlled structures due to the El Centro earthquake

Control Strategy / Response	Fixed Base	Low Damping Base Isolation	High Damping Base Isolation	Low Damping Base Isolation with MR Damper (voltage=0.5)	Low Damping Base Isolation with MR Damper (voltage=1.5)	Low Damping Base Isolation with MR Damper (voltage=2.25)
x_b	-	1.03	0.64	0.26	0.19	0.18
x_1	0.54	1.15	0.71	0.31	0.29	0.29
x_2	0.83	1.22	0.75	0.33	0.34	0.35
x_3 (cm)	0.97	1.26	0.77	0.34	0.39	0.39
d_b	-	1.03	0.64	0.26	0.19	0.18
d_1	0.54	0.13	0.08	0.09	0.15	0.16
d_2	0.32	0.07	0.05	0.08	0.10	0.11
d_3 (cm)	0.20	0.04	0.03	0.05	0.06	0.07
$\ddot{x}_b$	-	250	184	297	285	280
$\ddot{x}_1$	880	230	187	283	386	412
$\ddot{x}_2$	1065	242	167	240	325	332
$\ddot{x}_3$ (cm/s^2)	1412	285	191	365	474	478
f(N)	-	-	-	469	837	881

As shown in Table 4, adding low damping base isolation to the structure decreases the maximum response of fixed-base structure which in this case study the maximum drift and acceleration has about 76% and 80% reduction, respectively. Though using low damping base isolation has led to decrease the response of the structure, the base drift has been high. By using high damping base isolation, the maximum drift and acceleration of structure has been decreased about 85% and 86%. Also, the maximum base drift of low damping base isolation has been decreased about 38%. Therefore it can be said that using high damping base isolation could be suggested as an alternative to reduce the maximum base drift of the base isolated structures though its capability has been limited. An other alternative to decrease the maximum base drift is using MR damper in passive form with constant voltage that is linked between low damping base isolation and ground. In Table 4, the maximum response of the controlled structure has been given for different values of the voltage. From the results it is clear that using passive MR damper has caused the maximum base drift of the structure to be reduced, significantly. Also about 71% and 66% reduction has been achieved in the maximum drift and acceleration of the structure. Comparing the results

shows that using hybrid passive MR damper and low damping base isolation has been more effective in reducing the base drift in comparison with low and high damping base isolation.

6.2 Case (b): Designing optimal hybrid system of low damping base isolation and MR damper

In this section, the H_2/LQG and clipped-optimal control algorithm is applied to determine the voltage of the MR damper in each time step when the structure subjected to the scaled El Centro excitation. In Eq. (10), all elements of Q are zero, except for Q_{11}=1, this is because of the purpose of this paper that is minimizing the base drift. Also the optimal value of the weighting parameter, r, in Eq. (10) is determined using genetic algorithm without any limitation on the response. In design procedure only the weight parameter r is considered variable in H_2/LQG control and the objective function is defined as the minimization of the maximum base drift. Through solving the optimization problem using GA, the optimal value for r has been determined. In Figs. 6 and 7 the variations of the best fitness and fitness mean of individuals as well as the average distance between individuals have been shown during generations. It is clear that after a few number of generations the optimum answer has been found which shows the convergence behavior of the GA. For the optimum case, the maximum drift, acceleration, MR damper force and base drift of the controlled structure has been reported in Table 5. Also Figs. 8-10 shows time histories of the maximum response, MR damper voltage and force MR damper for different control systems. According to the results, when using semi-active base isolation about 84% reduction in maximum base drift has been achieved while the corresponding value has been about 38% for high base isolation system; hence it can be said that in designing optimal hybrid base isolation the main objective which has been minimizing the maximum base drift has been obtained. Also in this case the maximum drift and acceleration of the structure have been decreased about 72% and 68%, too, though the maximum acceleration has been increased in comparison with low and high damping base isolation. Hence, optimal design of hybrid MR damper and low damping base isolation has led to effective performance regarding controlling the base drift. Also this design procedure could be applied for designing effective hybrid base isolation to mitigate any desired response of the structure.

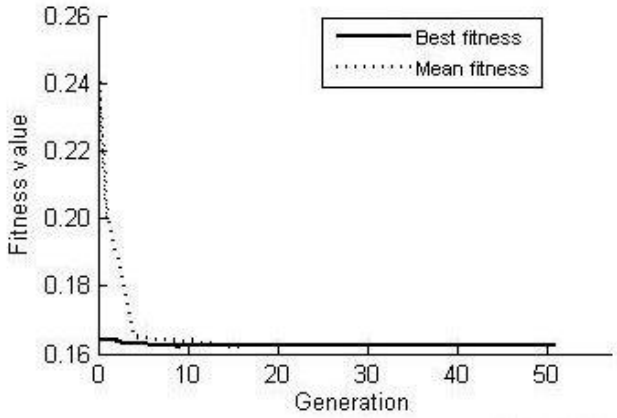

Figure 6. Best fitness and fitness mean during generations in GA

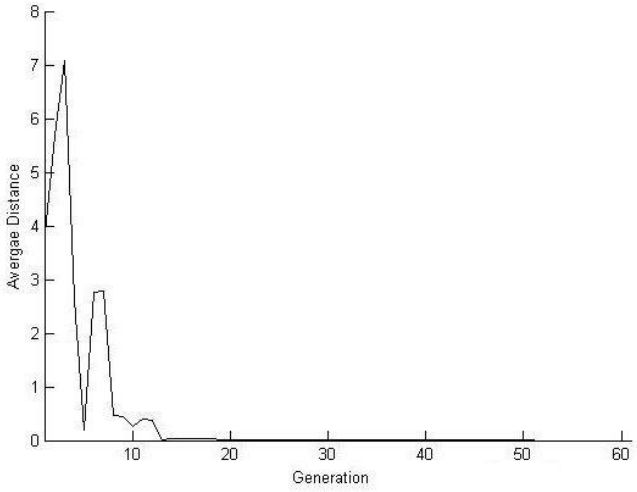

Figure 7. Average distance between individuals during generations in GA

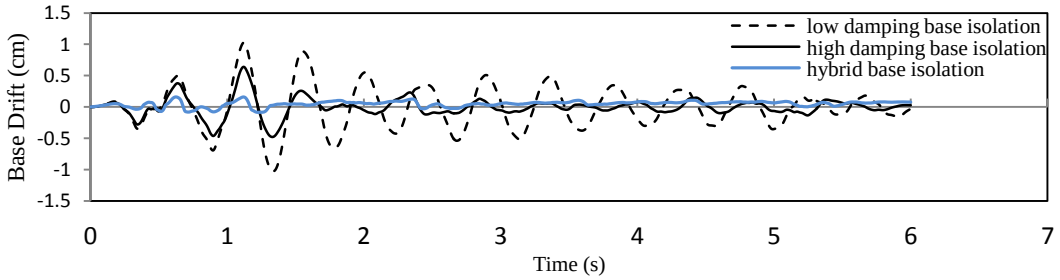

(a): Base drift

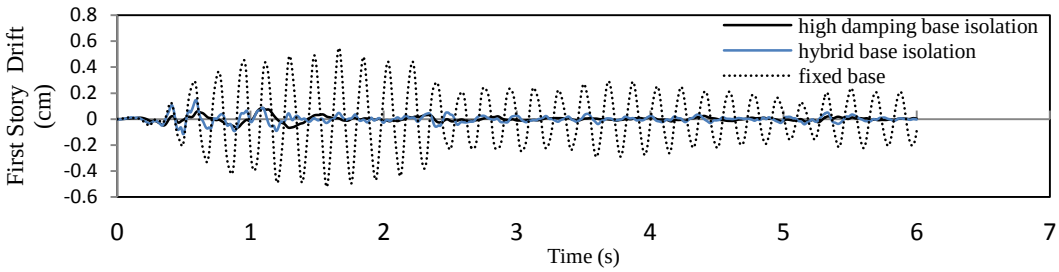

(b): First story drift

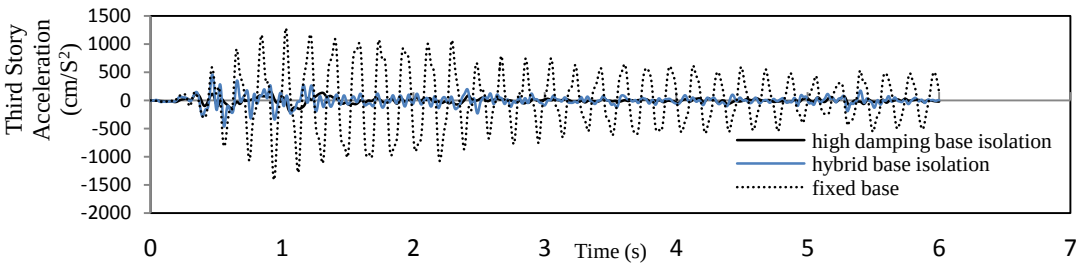

(c): Third story acceleration

Figure 8. Comparison of a) base drift, b) first story drift, and c) third story acceleration when using different base isolation control system

Applied voltage to the MR damper as shown in Fig. 9 considers only the maximum and minimum levels and changes between 0 and 2.25 (v).

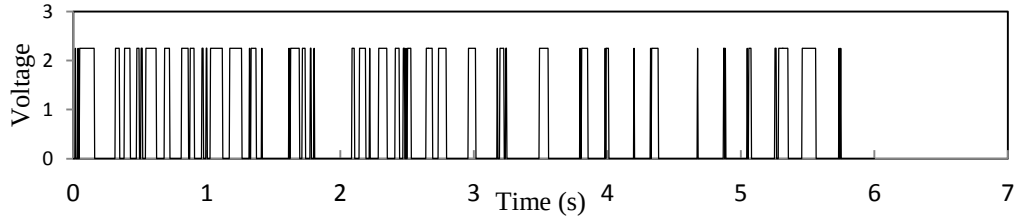

Figure 9. Applied voltage on the MR damper

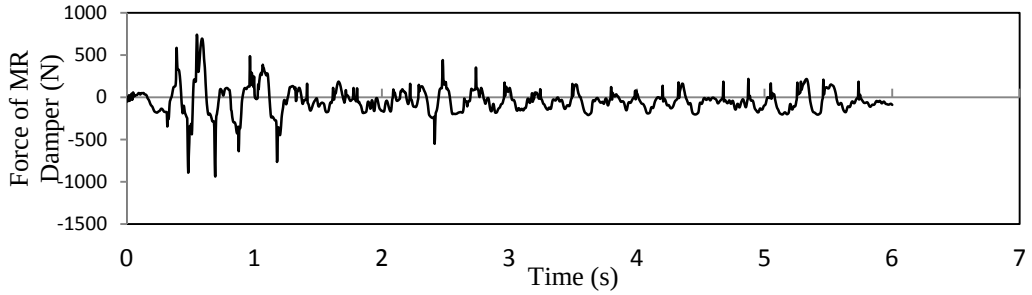

Figure 10. MR damper force

6.3 Case (c): Designing optimal constrained hybrid base isolation system

In *Case (b)* results have shown that when using hybrid base isolation, the maximum acceleration of the structure has been increased in comparison with low and high base isolation. Therefore in this section, in designing optimal hybrid system of low damping base isolation and MR damper, the maximum acceleration has been limited to the value obtained for third story (285 cm/s^2) which is the maximum value in low damping base isolation. In this case the optimization problem is solved to determine the optimal weighting parameter, *r*, while the constraint on the maximum acceleration is satisfied. For the optimal case the maximum response of structure has been shown in Table 5.

As shown in Table 5, the maximum acceleration of third story has been smaller than 285 cm/s^2; hence the constraint has been satisfied. The maximum base drift has been increased in comparison with the *Case (b)* though it is about 52% less than high damping base isolation. Therefore it can be concluded that it is possible to design optimal hybrid base isolation which has the capability of controlling the maximum drift, base drift and acceleration simultaneously.

6.4 Performance of optimal hybrid base isolation under testing excitations

In previous sections, the optimal hybrid system of MR damper and base isolation has been designed when the structure subjected to the El Centro earthquake. To assess the performance of optimal control systems under other excitations, the controlled structure using designed optimal hybrid base isolations of cases (b) and (c) subjected to the Northridge (PGA=0.58g, 1994) and the Tabas (PGA=0.85g, 1978) earthquake sand the results have been reported in Tables 6-7.

Table 5: Peak response of controlled structure due to the El Centro earthquake

Response \ Control Strategy	Hybrid Base Isolation-Case (b)	Hybrid Base Isolation-Case (c)
x_b	0.16	0.31
x_1	0.27	0.35
x_2	0.31	0.38
x_3	0.32	0.39
(cm)		
d_b	0.16	0.31
d_1	0.15	0.08
d_2	0.08	0.06
d_3	0.07	0.04
(cm)		
$\ddot{x}_b$	668	293
$\ddot{x}_1$	478	246
$\ddot{x}_2$	376	237
$\ddot{x}_3$	461	284
(cm/s^2)		
f(N)	938	292

Table 6: Peak response of uncontrolled and controlled structures due to the Northridge earthquake

Response \ Control Strategy	Fixed Base	Low Damping Base Isolation	High Damping Base Isolation	Hybrid Base Isolation-Case (b)	Hybrid Base Isolation-Case (c)
x_b	-	1.34	0.74	0.29	0.28
x_1	0.59	1.5	0.84	0.43	0.36
x_2	0.85	1.58	0.89	0.52	0.41
x_3	0.99	1.62	0.93	0.61	0.43
(cm)					
d_b	-	1.34	0.74	0.29	0.28
d_1	0.59	0.17	0.11	0.20	0.12
d_2	0.33	0.09	0.06	0.12	0.06
d_3	0.28	0.05	0.04	0.10	0.08
(cm)					
$\ddot{x}_b$	-	303	224	757	780
$\ddot{x}_1$	1527	308	258	764	521
$\ddot{x}_2$	1385	316	227	491	325
$\ddot{x}_3$	1950	370	285	702	548
(cm/s^2)					
f(N)	-	-	-	1474	619

Table 7: Peak response of uncontrolled and controlled structures due to the Tabas earthquake

Response \ Control Strategy	Fixed Base	Low Damping Base Isolation	High Damping Base Isolation	Hybrid Base Isolation-Case (b)	Hybrid Base Isolation-Case (c)
x_b	-	2.5	1.21	0.47	0.56
x_1	0.93	2.8	1.36	0.63	0.65
x_2	1.47	2.9	1.44	0.71	0.67
x_3 (cm)	1.73	3	1.48	0.78	0.69
d_b	-	2.5	1.21	0.47	0.56
d_1	0.93	0.3	0.18	0.24	0.14
d_2	0.53	0.15	0.11	0.14	0.11
d_3 (cm)	0.32	0.08	0.07	0.09	0.08
$\ddot{x}_b$	-	514	414	1324	3105
$\ddot{x}_1$	1409	530	394	734	434
$\ddot{x}_2$	1942	553	360	730	364
$\ddot{x}_3$ (cm/s^2)	2202	574	460	658	596
f(N)	-	-	-	3000	3000

According to the results it is clear that under testing excitations the hybrid base isolation system has been more effective than high damping base isolation in mitigating the maximum base drift which is the main objective in designing procedure.

7. CONCLUSIONS

In this paper optimal design of hybrid low damping base isolation with MR damper and assess its performance in mitigating the response of structures has been studied. The main objective of this research has been designing optimal hybrid base isolation which has the capability of controlling the maximum base drift of low damping base isolation. To this end, optimal semi-active base isolations using MR damper have been designed where the H_2/LQG and clipped-optimal control algorithm has been used to determine the voltage of MR damper. A three-story frame subjected to the scaled El Centro excitation and optimal hybrid base isolations have been designed which genetic algorithm (GA) has been used to determine the weighting parameter in H_2/LQR algorithm. Also the performance of three types of passive base isolation systems including low damping, high damping and hybrid base isolation with constant voltage MR damper has been studied. Results of numerical simulations has shown that hybrid base isolation has been more effective than high damping base isolation system in controlling the maximum base drift of the structure so that in this case study about 75% more reduction in maximum base drift has been obtained by using the hybrid base isolation. Also it has been found that for reducing the maximum acceleration of

structure when using hybrid base isolation, it is possible to consider constraint on maximum acceleration in optimization procedure. Testing the optimal hybrid base isolations as well as low and high damping base isolations under excitations which are different from design record in characteristics has shown that optimal hybrid systems has been more effective in controlling the maximum drift of the structure and the base drift. Therefore, semi-active optimal hybrid base isolation control system designed according the procedure of this research could be suggested as an efficient control system for controlling the response of the structures and also to overcome the shortcoming of low damping base isolations regarding the maximum base drift.

REFERENCES

1. Naeim F, Kelly JM. *Design of Seismic Isolated Structure: From Theory to Practice*, Wiley, England, 1999.
2. Taylor DP, Constantinou MC. Fluid dampers for application of seismic energy dissipation and seismic isolation, Tech. Rep., Taylor Devices, Inc., North Tonawanda N.Y, 2000.
3. Inaudi JA, Kelly JM. Hybrid isolation systems for equipment protection, *Earthquake Eng Struct Dynam* 1993; **22**(4): 297-313.
4. Yang JN, Wu JC, Reinhorn AM, Riley M. Control of sliding-isolated buildings using sliding-mode control, *ASCE J Struct Eng* 1996; **122**(2): 179-86.
5. Nagarajaiah S, Riley M, Reinhorn A. Control of sliding-isolated bridge with absolute acceleration feedback, *ASCE J Eng Mech* 1993; **119**(11): 2317-32.
6. Yoshioka H, Ramallo SC, Spencer BF. Smart base isolation strategies employing Magnetorheological Dampers, *ASCE J Eng Mech* 2002; **128**(5): 540-51.
7. Dyke SJ, Wang Y. Modal-base LQG for smart base isolation system design in seismic response control, *Struct Control Health* 2013; **20**(20):753-68.
8. Bo Chen, Yu-zhou S, Yong-le L, Sheng-lin Z. Control of seismic response of a building frame by using hybrid system with magnetorheological dampers and isolators, *Adv Struct Eng* 2014; **17**(8): 1199-1216.
9. Bagherkhani A, Mohebbi M. Optimal design of magneto-rheological dampers, *Int J Optim Civil Eng* 2014; **4**(3): 361-80.
10. Ghasemi MR, Barghi E. Estimation of inverse dynamic behavior of MR dampers using artificial and fuzzy-based neural networks, *Int J Optim Civil Eng* 2012; **2**(3): 357-68.
11. Ramallo JC, Spencer BF, Johnson EA. Smart base isolation systems, *ASCE J Eng Mech* 2002; **128**(10): 1088-99.
12. Sanjay S, Nagarajaiah S. Experimental study of sliding base-isolation buildings with Magneto-rheological Dampers in near-fault earthquake, *ASCE J Struct Eng* 2005; **131**(7): 1025-34.
13. Yongfeng DU, Xiang Z, Guanghuan W. Collapse simulation of plan irregular isolation structures subjected to near-fault seismic motion, *Appl Mech Mater* 2013; **433**: 2290-94.
14. Dyke SJ, Spencer BF, Sain MK, Carlson JD. Modeling and control of Magnetorheological dampers for seismic response reduction, *Smart Mater Struct* 1996; **5**(5): 565-75.
15. Dyke SJ, Spencer BF, Sain MK, Carlson JD. Phenomenological model of a Magneto-rheological damper, *ASCE J Eng Mech* 1997; **123**(3): 230-38.
16. Bani-Hani K, Sheban M. Semi-active neuro-control for base-isolation system using magnetorheological dampers, *Earthquake Eng Struct Dynam* 2006; **35**(9): 1119-44.

17. Dyke SJ, Jansen LM. Semi-active control strategies for MR damper: A comparative study, *J Eng Mech* 2000; **126**(8): 795-803.
18. Baker JE. Reducing bias and inefficiency in the selection algorithm, *Proceeding of 2nd International Conference on Genetic Algorithm (ICGA)*, Cambridge, MA, USA, 1987, pp. 14-21.
19. Muhlenbein H, Schlierkamp-Voosen D. Predictive models for the breeder genetic algorithm: I. continuous parameter optimization, *Evol Comput* 1993; **1**(1): 25-49.
20. Zahedi Tajrishi F, Mirza Goltabar Roshan AR. Optimal sensor placement for modal identification of a strap-braced cold formed steel frame based on improved genetic algorithm, *Int J Optim Civil Eng* 2014; **4**(1): 93-119.
21. Shakeri K. Optimum weighted mode combination for nonlinear static analysis of structures, *Int J Optim Civil Eng* 2013; **3**(2): 245-57.
22. Arfiadi Y, Hadi MNS. Optimum placement and properties of tuned mass dampers using hybrid genetic algorithms, *Int J Optim Civil Eng* 2011; **1**(1): 167-87.
23. Mohebbi M. Minimizing Hankel's Norm as design criterion of multiple tuned mass dampers, *Int J Optim Civil Eng* 2013; **3**(2): 271-88.
24. Mohebbi M, Moradpour S, Ghanbarpour Y. Improving the seismic response of nonlinear steel structures using optimal MTMDs, *Int J Optim Civil Eng* 2014; **4**(1): 137-50.
25. Villaverde R. *Fundamental concepts of earthquake engineering*, 978-1-4200-6495-7, Taylor and Francis group, USA, 2009.